

MURI Research Center for Intelligent Design and
Manufacturing in Electronics and Materials

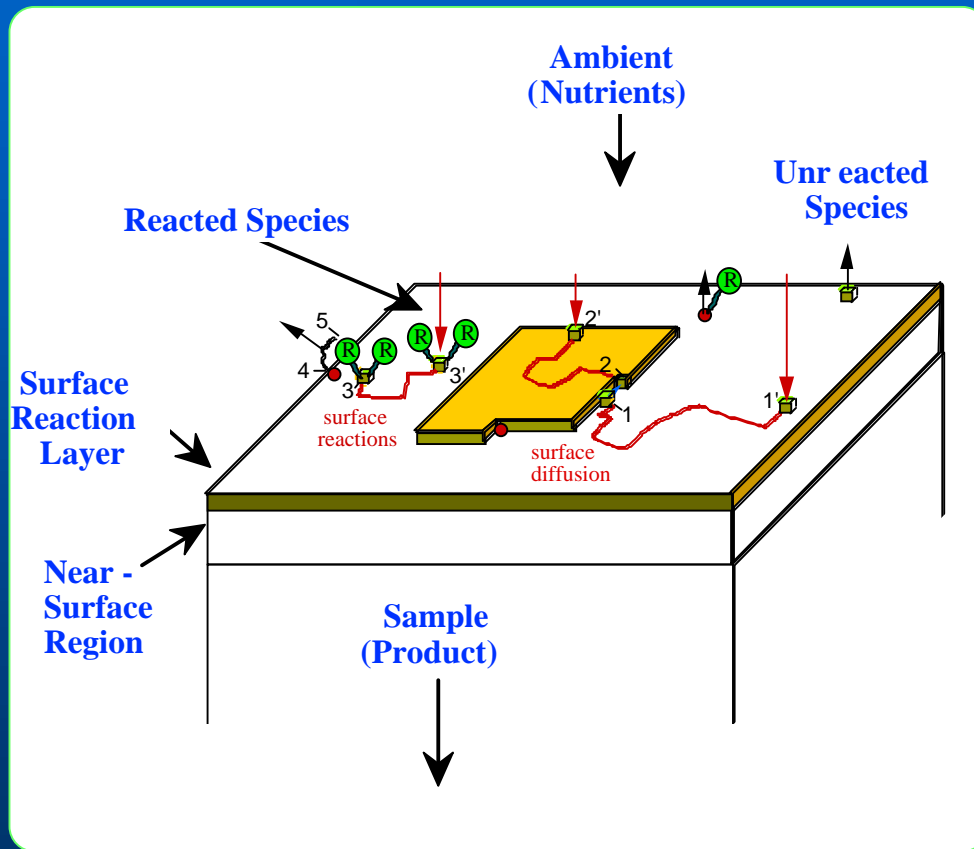
**Modeling and Control of Advanced CVD
Processes: The Control of Defects in III-V
Compound Heterostructures**



NC STATE University

ASU™ ARIZONA STATE
UNIVERSITY

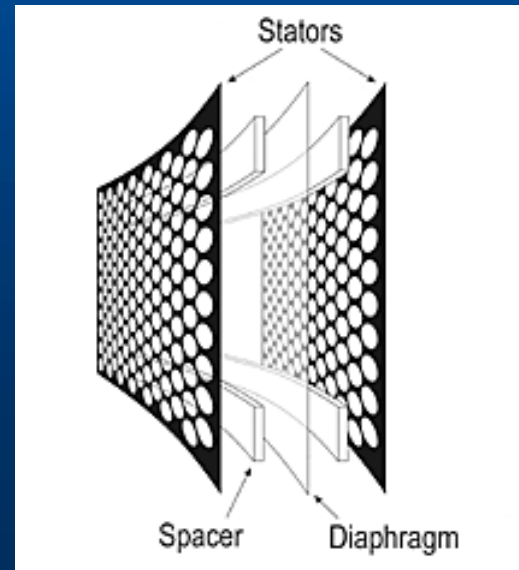
Chemical Vapor Deposition (CVD)?



- CVD process uses **chemically reacting gases** to form a thin solid film with controllable properties (e.g., film composition and thickness)
- Reactions occur in both the gas phase and in the region on top of the film (SRL)
- Deposition process is driven **thermally** by heating the substrate (500-1000°C)

Applications of CVD

- Widely used in the **microelectronics industry** for the fabrication of
 - High-speed IC (GaAs), transistors, memory chips (DRAM)
- Used in **UV detectors** and green and blue **LEDs**
- Also used in the manufacturing of **electrostatic loudspeakers (ESL)**
 - Martin-Logan ESL



Why a High-Pressure CVD Reactor?

- **High partial pressure** of the group V precursors is desirable for **control** of native point defect chemistry and **doping** of III-V materials
- **High pressure** is necessary for the production of some materials (such as InN) in a **desirable temperature range**
- **High throughput** as a result of high pressure is an essential requirement of competitive single-wafer semiconductor processing



Trade-off between these benefits and the
difficulty of real-time process control

Team Members

Participants supported under MURI and associated AASERTs

FACULTY

K.J. Bachmann
H.T. Banks
N. Dietz
K. Ito
M. Kushner

G. Lucovsky
S. Mahajan
J.S. Scroggs
H.T. Tran
H. Yang

POSTDOCS

H.V. Ly (*Cal. State at Fullerton*)
G. Pinter (*Univ. of Wisc. at Milwaukee*)
I. Lauko (*Univ. of Wisc. at Milwaukee*)
S. Ravindran (*Univ. of Alabama at Huntsville*)
R. del Rosario (*Univ. of the Philippines at Diliman*)

F. Schienle (*Aixtron*)
F. Wang
M. Fang (*Tomphson*)
C. Hoepfner (*Spire Inc.*)
G.M. Kepler

Team Members (*continue*)

STUDENTS

D. Cronin

C. Harris (*MS, July 99*)

E. Keiter

R. Kinder

R. Johnson

S. LeSure

J. Lu

S. McCall

V.J. Narayanan

E.H. Sanchez

J. Schroeter (*PhD, December 98, EPA*)

T. Simon (*PhD, March 99, Intelligent Sys.*)

D. Stephens

N. Sukidi (*PhD, March 98, Motorola*)

S.C. Beeler (*PhD, October 00*)

A.N. Westmeyer

D. Wolfe

V. Woods (*MS, March 00, Microcoating
Technology, Inc.*)

N. Young

D. Zhang

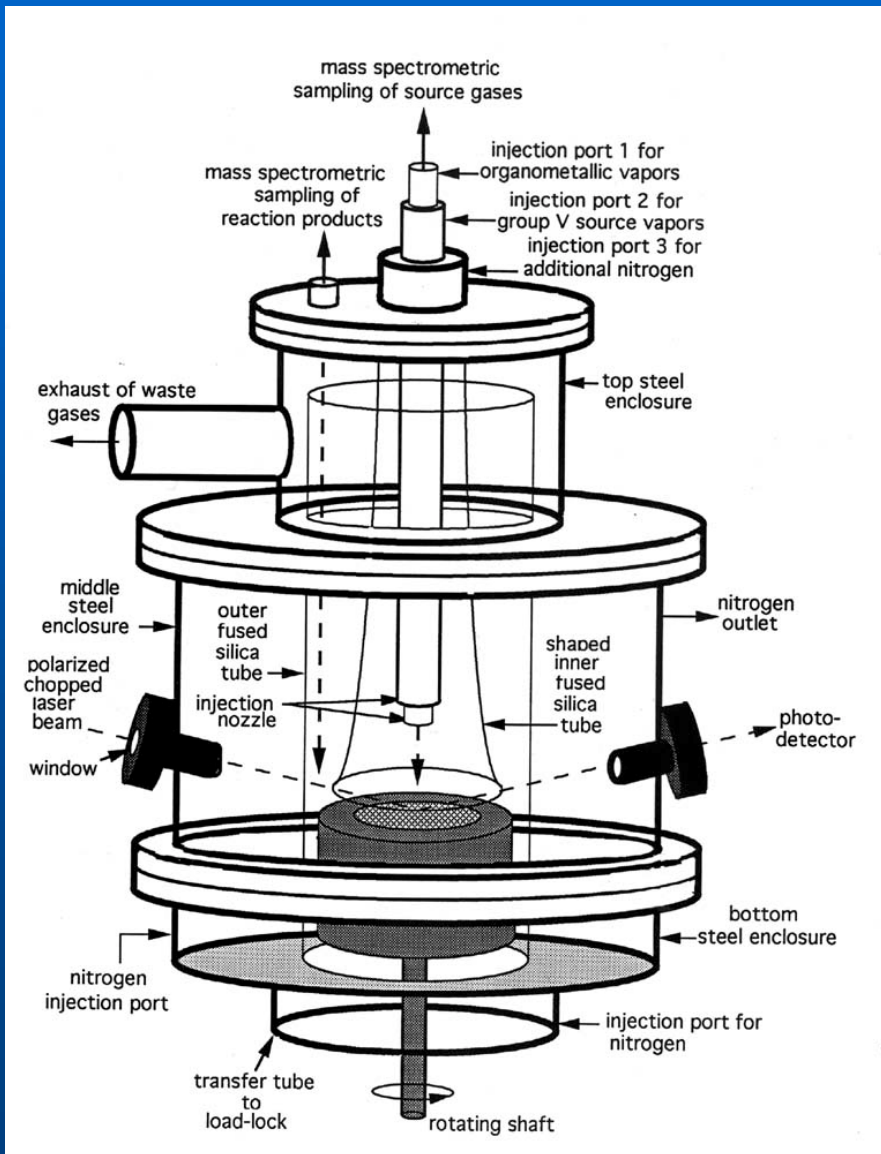


Computer Aided Modeling, and Reactor Design History

Design reactors with

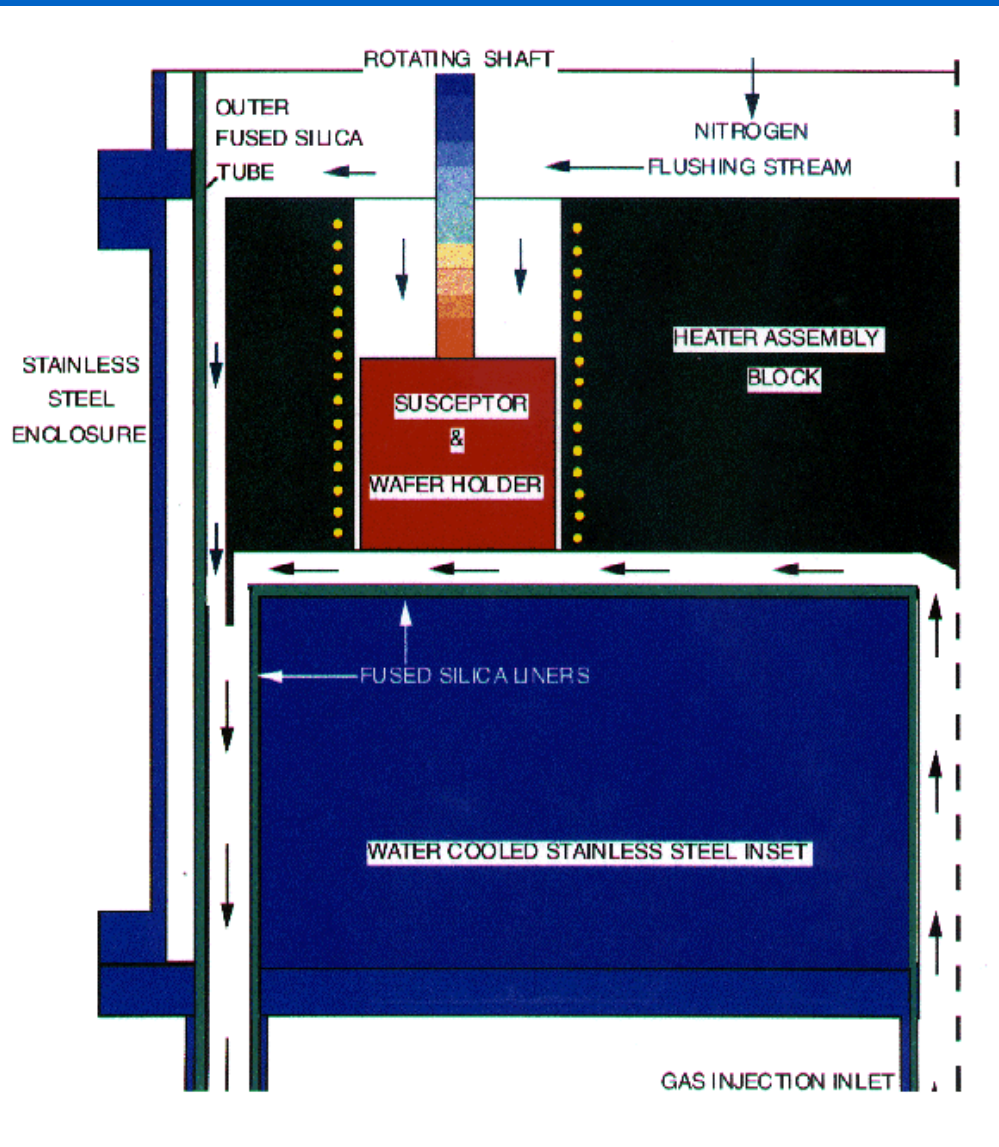
- **Implementable real-time sensing**
- **Real-time controllability**

First Generation Reactor Design

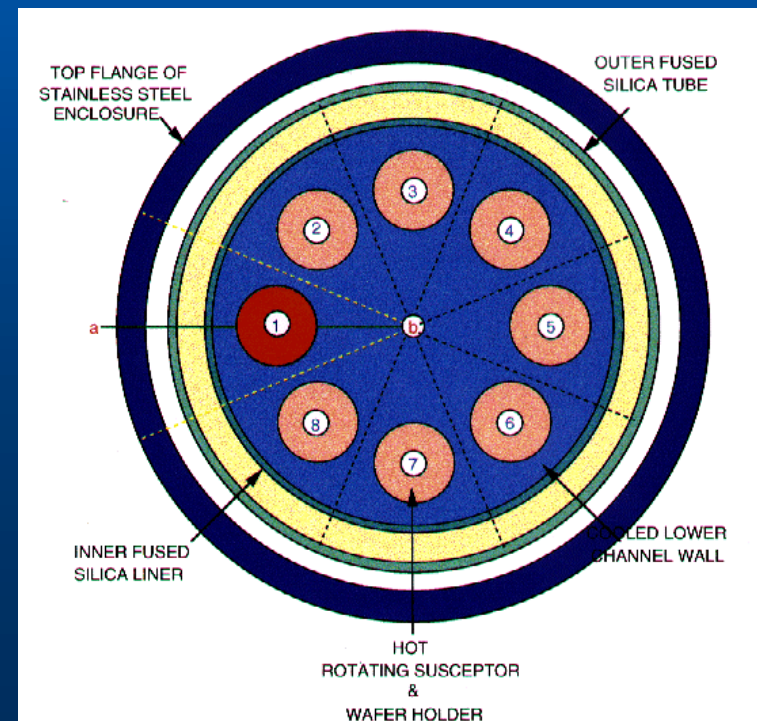


- **Recirculation cells develop at the outer edges of the substrate**

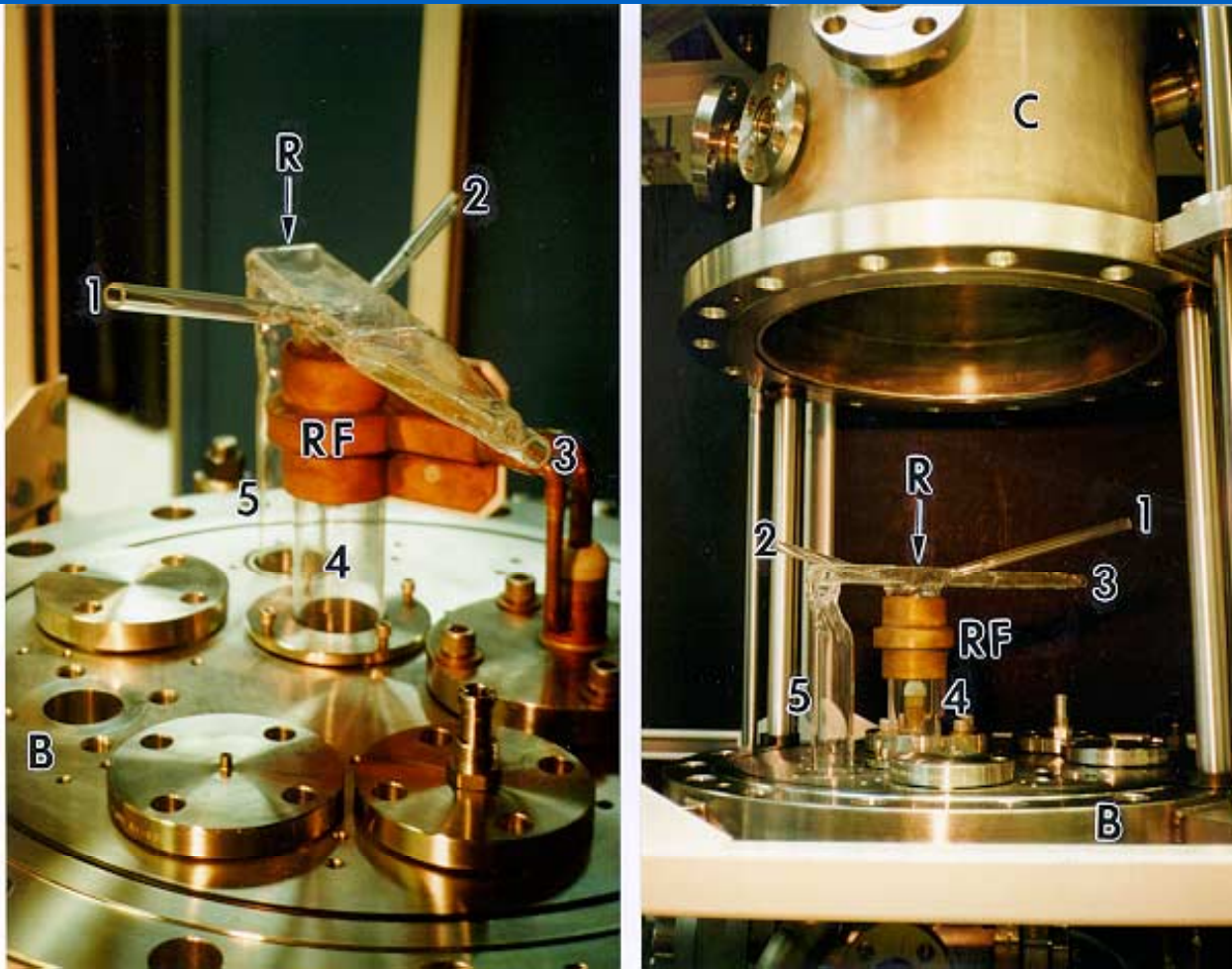
Second Generation Reactor Design



- Substrate is moved away from the impinging jet
- Horizontal flow across the substrate
- Multiple wafers capability



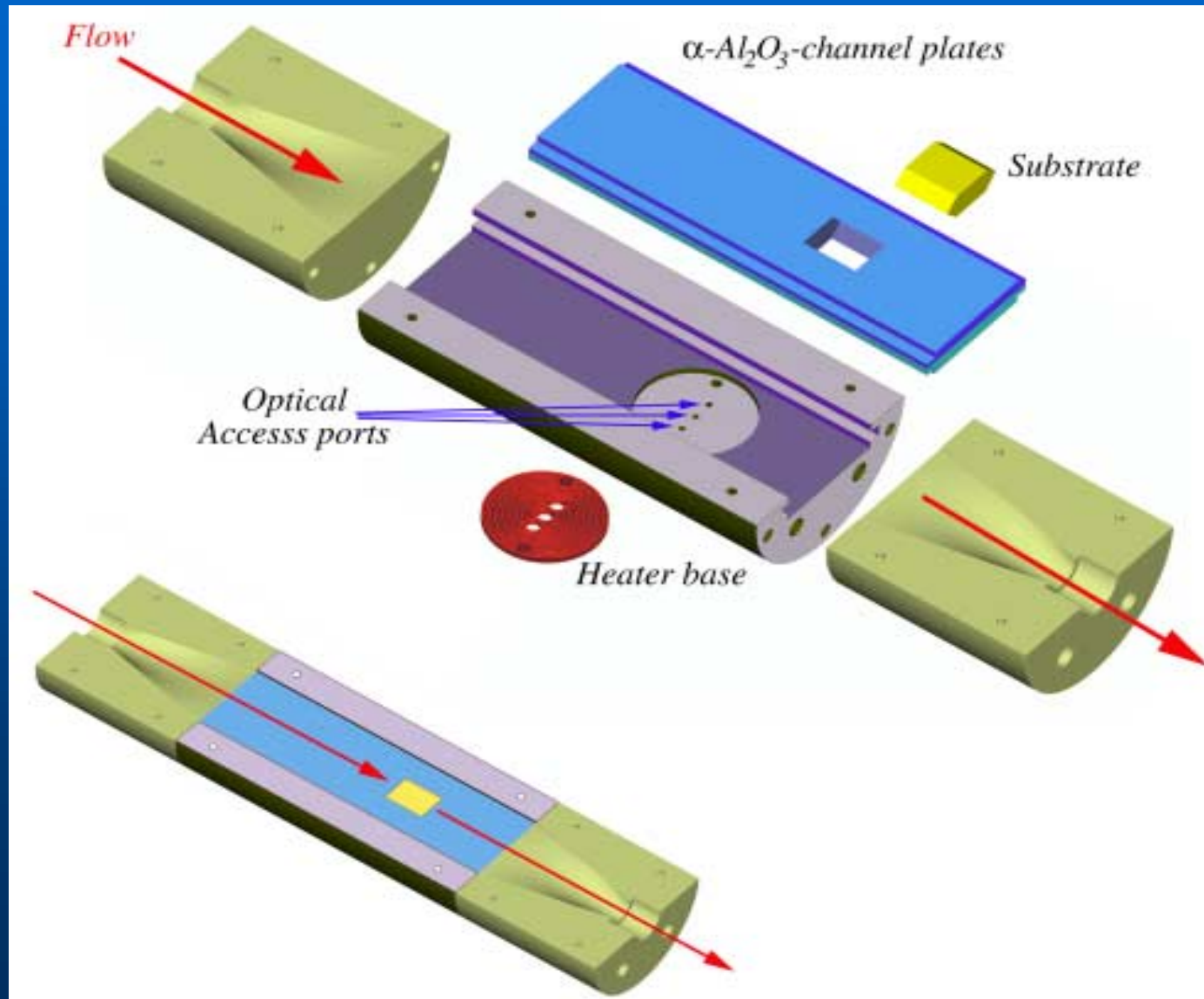
Third Generation Reactor Design



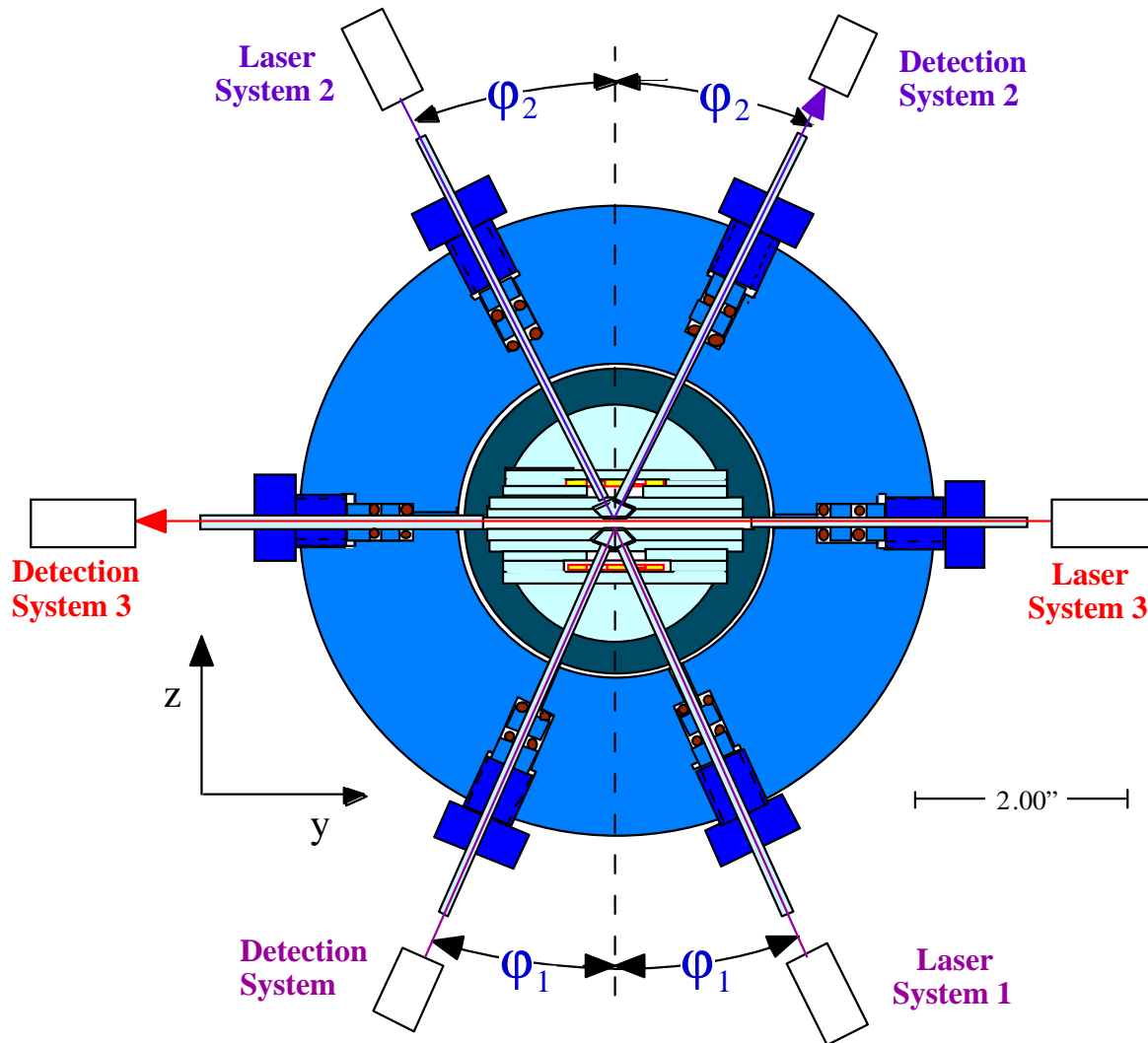
- Differentially Pressure Controlled (DPC) reactor system (5 atm)
- Fused silica reactor with tubular connections to load lock, windows for PRS, gas injection and exhaust
- Stainless steel second confinement shell
- R = fused silica reactor
1&2 = win. connectors
C = confinement shell
3&5 = gas inlet & outlet
4 = tube on R for substrate wafer exchange

Fourth Generation Reactor Design

- Pressure range (up to **100 atm**)
- Constant cross section
- **Small channel height** (1mm)
- Symmetric substrate arrangement
- Elimination of competitive polycrystalline deposition
- Improved reactor efficiency



Real-Time Film Growth Sensing



Gas phase monitoring

– Absorption Spectroscopy

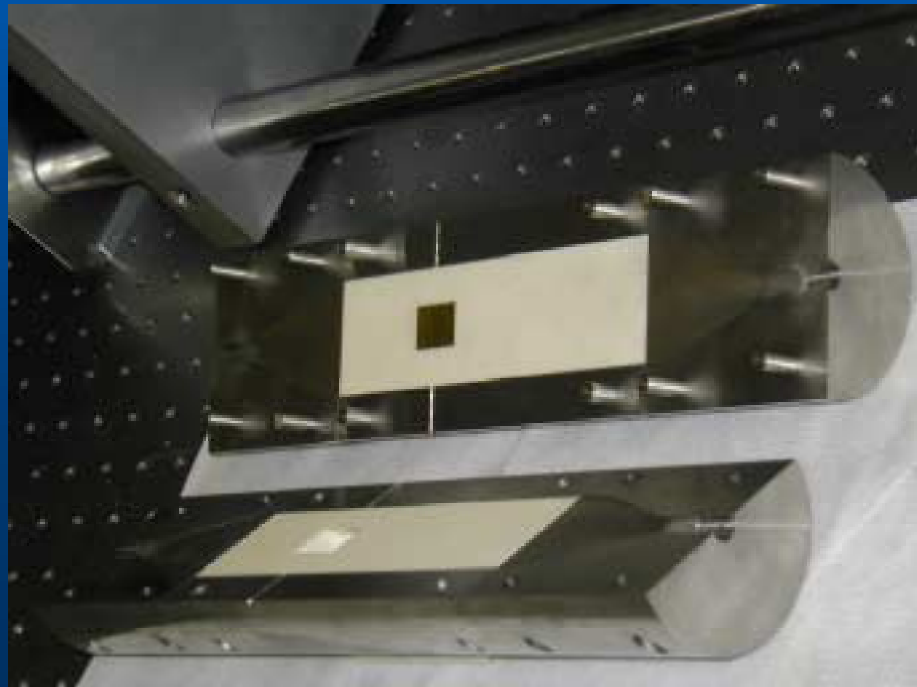
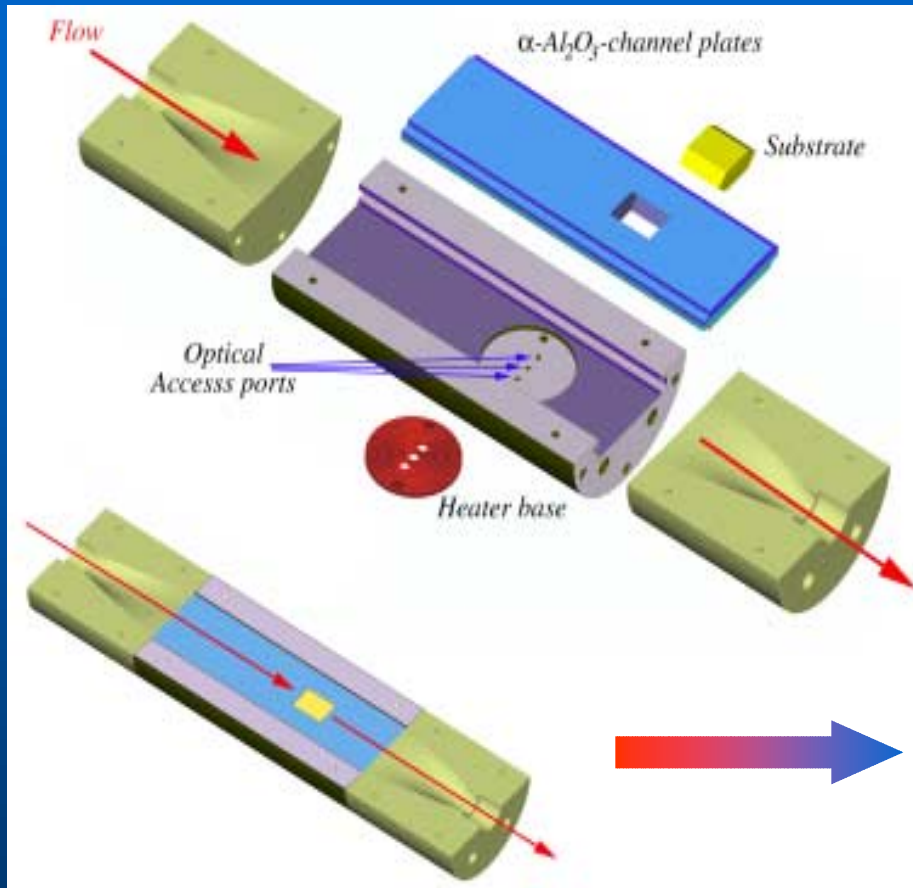
Nucleation kinetics and heteroepitaxial overgrowth monitoring

– Principle Angle Spectroscopy (PAR)

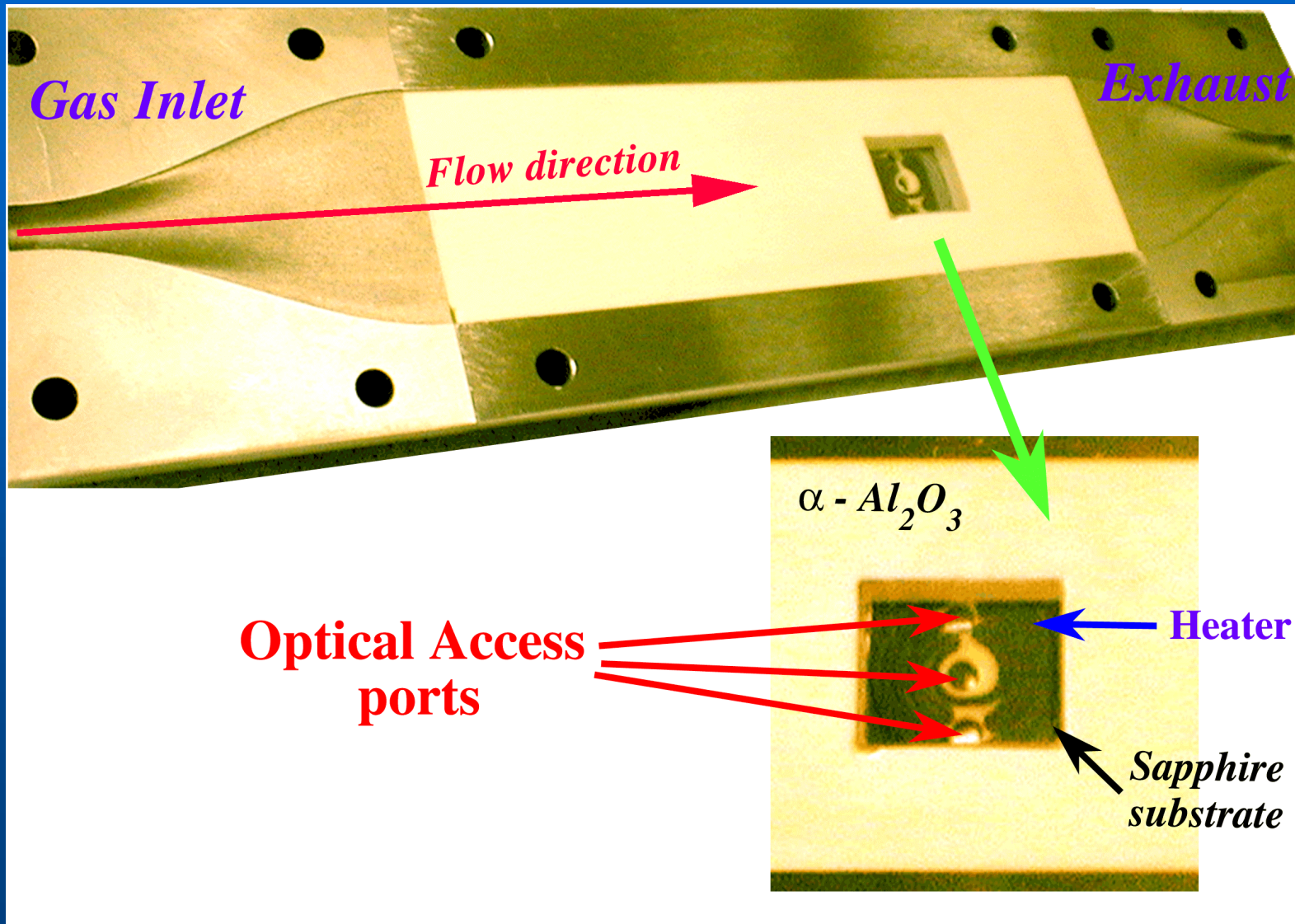
Fourth Generation Reactor



Fourth Generation Reactor



Fourth Generation Reactor



Real-Time Feedback Control of CVD Reactor

Nonlinear Measurements

REAL-TIME PROCESS SENSING

INPUT

- Flow rates
- Source vapor pulse profiles

CHAMBER

- Continuity
- Momentum
- Energy
- Species
- Eqn. Of State

DEPOSITION PROCESS

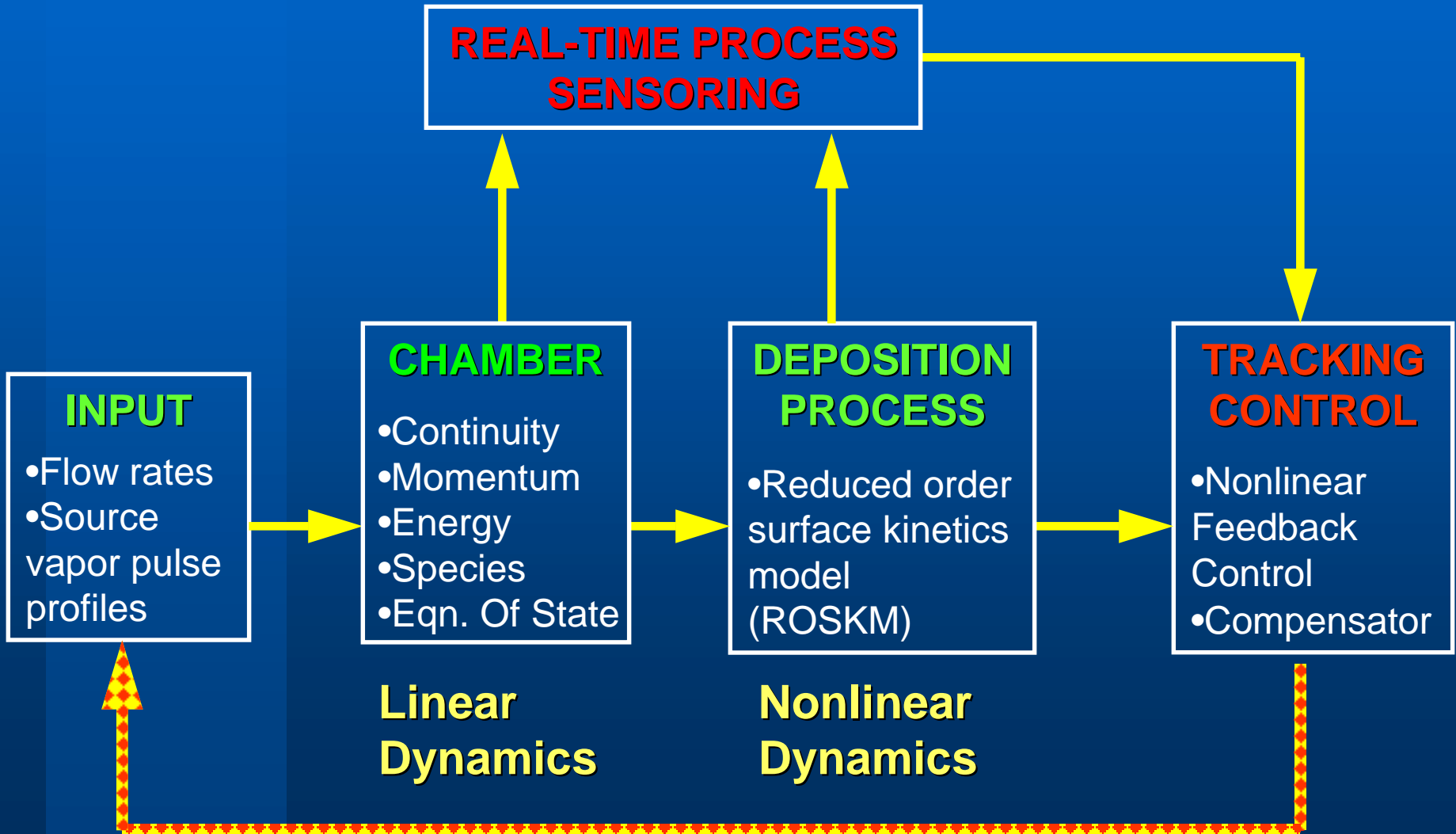
- Reduced order surface kinetics model (ROSKM)

TRACKING CONTROL

- Nonlinear Feedback Control
- Compensator

Linear Dynamics

Nonlinear Dynamics



Challenges & Approaches

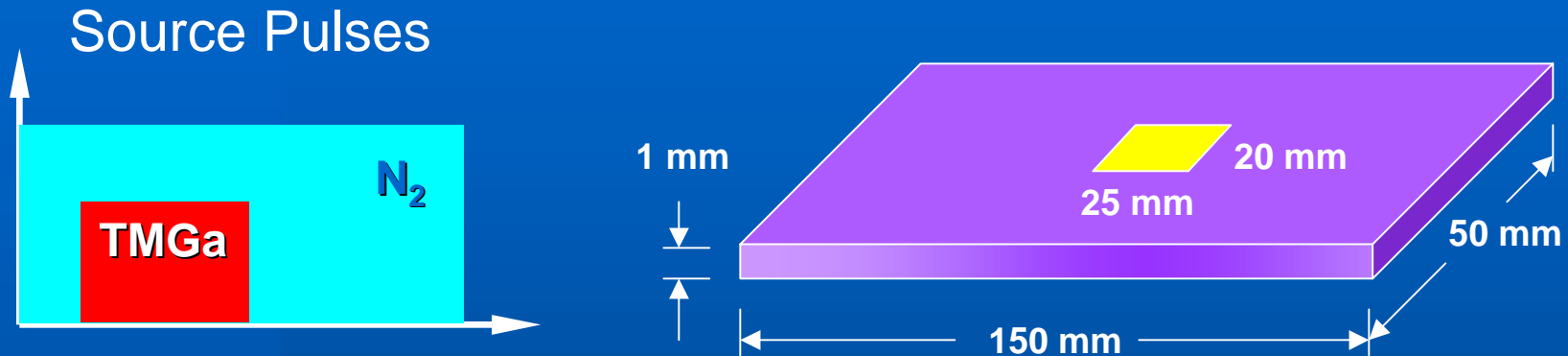
CHALLENGES

- Infinite Dimensional System (Nonlinear Dynamics)
- Dirichlet Boundary Control
- Nonlinear Tracking Control
- Nonlinear Partial State Observation

APPROACHES

- Reduced Order Model (POD)
- Penalty Boundary Formulation (Neumann Boundary Control)
- SDRE
- Nonlinear State Estimator

Problem Formulation



- All fluid and mass transport parameters are **temperature dependent**
- Only a trace amount of reactant compounds mixed with carrier gas is used
- Gas flow is **steady** (but **mass transport equation is time dependent**)

Quasi-Transient Flow

Continuity: $\nabla \cdot (\rho \vec{u}) = 0$


Eqn. Of State: $\rho = \rho_0 [1 - \beta_T (T - T_0)]$

Momentum: $\rho \vec{u} \cdot \nabla \vec{u} = -\nabla P + \nabla \cdot \sigma + (\rho - \rho_0) \vec{g}$

$$\sigma = -\frac{2}{3} \mu (\nabla \cdot \vec{u}) \vec{I} + \mu (\nabla \vec{u} + \nabla \vec{u}^T)$$

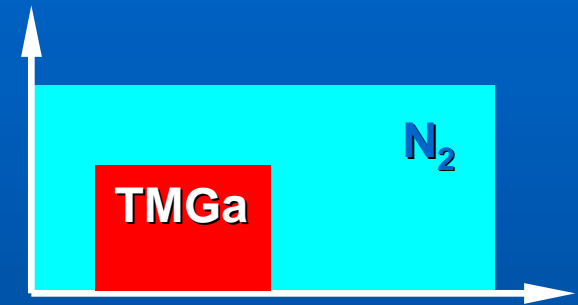
Energy: $c_p \rho \vec{u} \cdot \nabla T = \nabla \cdot (k_T \nabla T)$

Species: $\frac{\partial c_i}{\partial t} + \vec{u} \cdot \nabla c_i = \frac{1}{\rho} \nabla \cdot (\rho D_i \nabla c_i) + \sum_{i=1}^{N_R} r_{ni}$



Gas-Phase Reaction

TMGa: $\text{Ga}(\text{CH}_3)_3$ (N_2 carrier gas, 1000°K substrate temp, **10 atm**)




Reaction rates (Arrhenius' law):


$$r_i = \gamma_{ni} e^{-E_{ni}/RT} c_{ni}, \quad n = \text{TMGa, DMGa, MMGa}$$



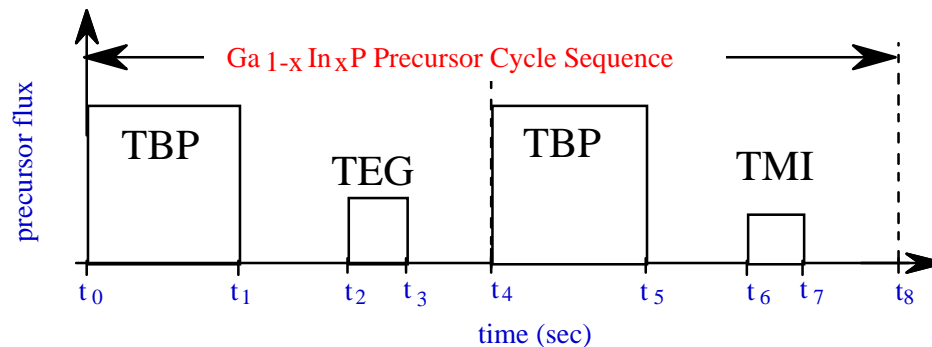
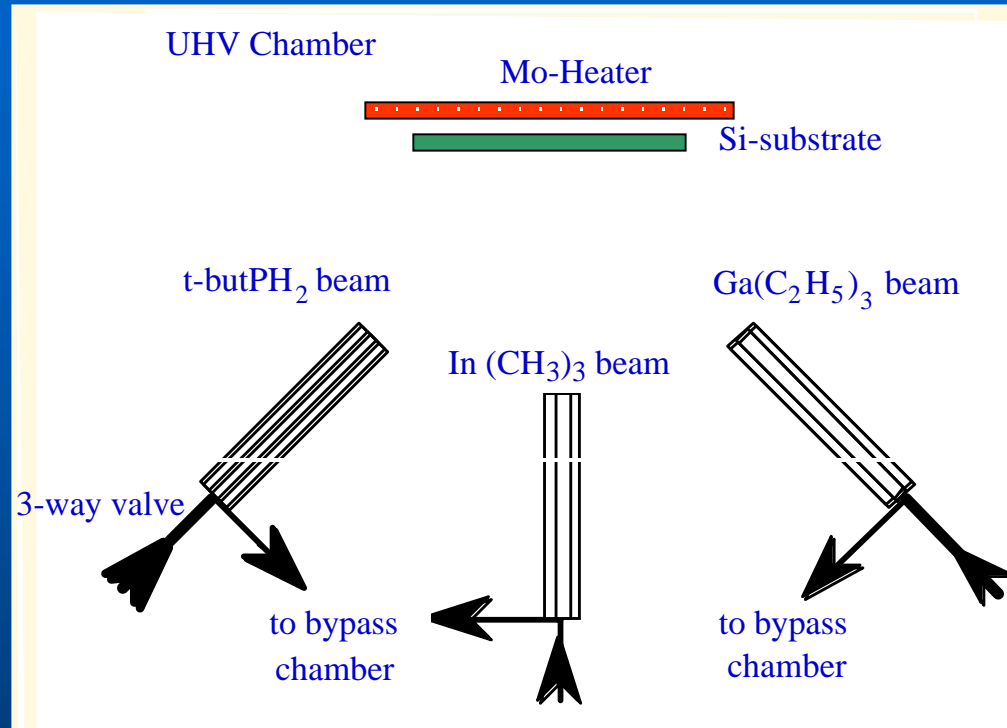
3 species: $\text{Ga}(\text{CH}_3)_3$, $\text{Ga}(\text{CH}_3)_2$, and GaCH_3



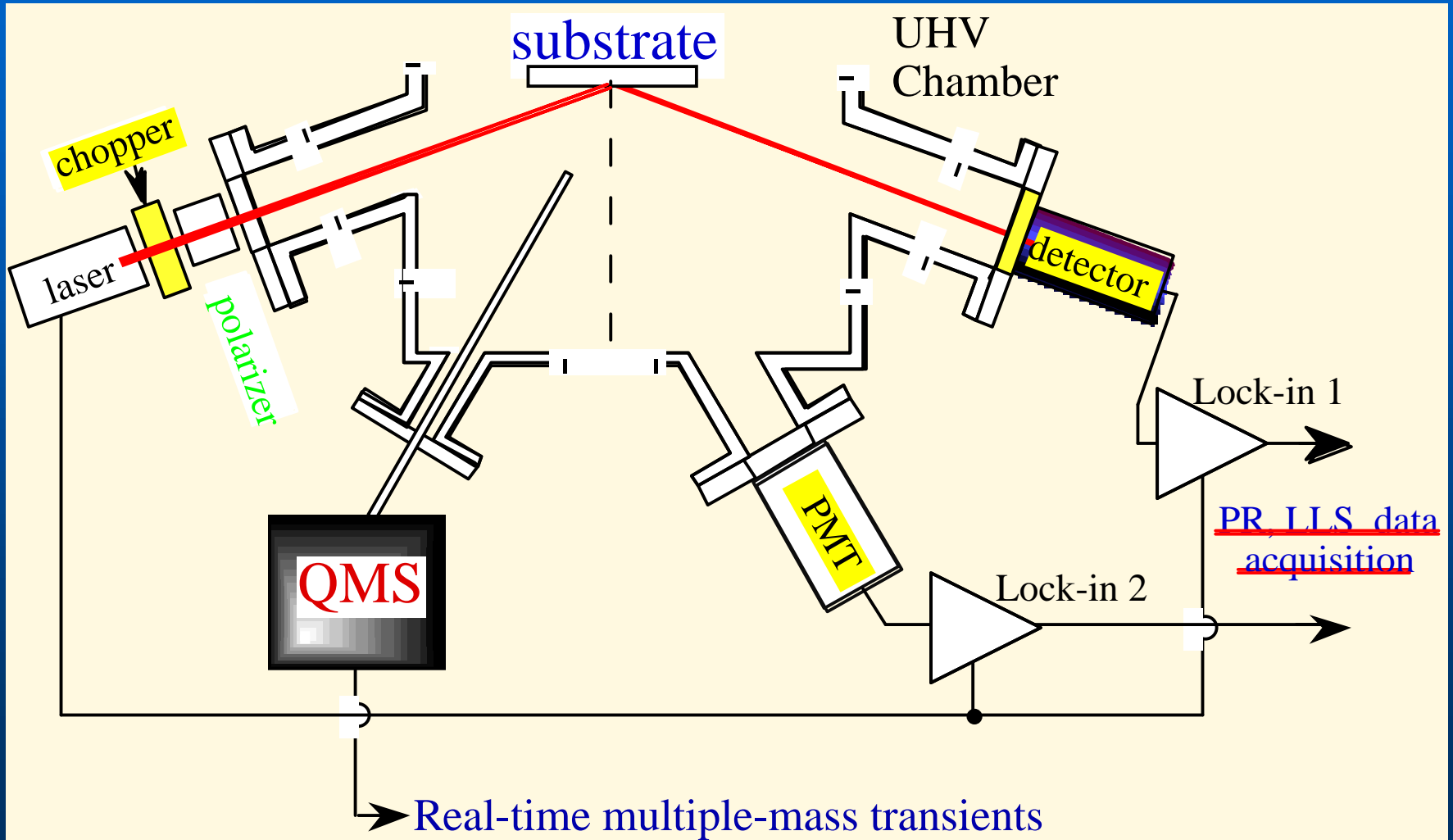
Real Time Monitoring
by
P-Polarized Reflectance Spectroscopy
(PRS)



Pulsed Chemical Beam Epitaxy (PCBE)

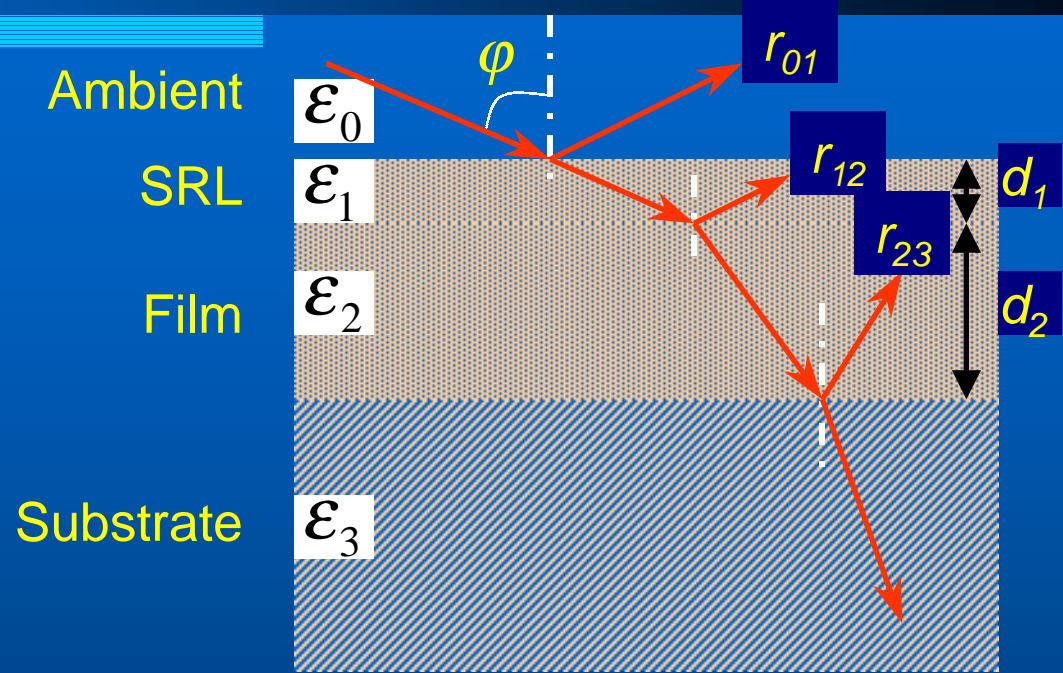


Experimental Arrangement



PRS: Fine Structure Modeling

Fresnel's
equation for the
four layer stack



Reflectance coefficient:

$$r = \frac{r_{01} + r_{12}e^{-2i\phi_1} + r_{23}e^{-2i(\phi_1+\phi_2)} + r_{01}r_{12}r_{23}e^{-2i\phi_2}}{1 + r_{01}r_{12}e^{-2i\phi_1} + r_{01}r_{23}e^{-2i(\phi_1+\phi_2)} + r_{12}r_{23}e^{-2i\phi_2}}$$

$$\phi_1 = \frac{2\pi d_1}{\lambda} \sqrt{\epsilon_1 - \epsilon_0 \sin^2 \phi}$$

d_1 - average SRL thickness

d_2 - film thickness

$$\phi_2 = \frac{2\pi d_2}{\lambda} \sqrt{\epsilon_2 - \epsilon_0 \sin^2 \phi}$$

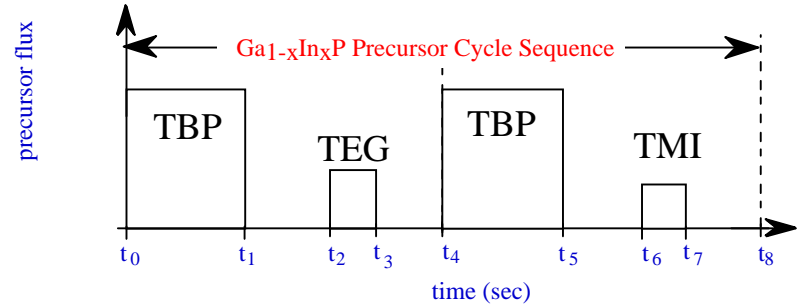
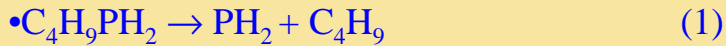
ϵ_1 - effective dielectric function of SRL

ϵ_2 - dielectric function of film

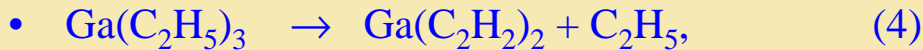
Reduced Order Surface Kinetics (ROSK)

Model for $\text{Ga}_{1-x}\text{In}_x\text{P}$ Growth

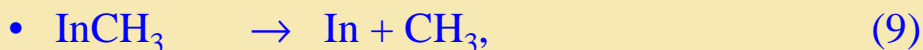
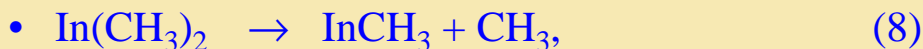
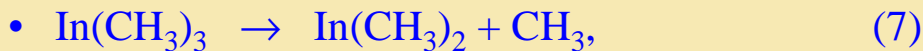
Thermal decomposition of TBP: for Si(001)



TEG pyrolysis:



TMI pyrolysis:



We assume one dominant reaction for the first precursor (TBP) and two dominant reactions for the second and third precursors (TEG and TMI). The SRL is treated as an homogenous ideal solution and the surface area is simplified to be constant.

ROSK Model

Simplified first precursor
(TBP) approximation:

$$\frac{d}{dt}n_1(t) = n_{\text{TBP}} - \tilde{a}_1 n_1(t) - \tilde{a}_4 n_3(t) n_1(t) - \tilde{a}_7 n_6(t) n_1(t)$$

Approximate second precursor
(TEG) reactions:

$$\frac{d}{dt}n_2(t) = n_{\text{TEG}} - \tilde{a}_2 n_2(t)$$

$$\frac{d}{dt}n_3(t) = \tilde{a}_2 n_2(t) - \tilde{a}_3 n_3(t) - \tilde{a}_4 n_3(t) n_1(t)$$

Simplified third precursor
(TMI) reactions approximation:

$$\frac{d}{dt}n_5(t) = n_{\text{TMI}} - \tilde{a}_5 n_5(t)$$

$$\frac{d}{dt}n_6(t) = \tilde{a}_5 n_5(t) - \tilde{a}_6 n_6(t) - \tilde{a}_7 n_6(t) n_1(t)$$

Two incorporation reactions:
(for GaP and InP, respectively)

$$\frac{d}{dt}n_{\text{GaP}}(t) = \tilde{a}_4 n_3(t) n_1(t) \quad \text{and} \quad \frac{d}{dt}n_{\text{InP}}(t) = \tilde{a}_7 n_6(t) n_1(t)$$

Note: Surface structure, number of reaction sides and inhomogeneous reactions are approximated at this point in the reaction parameters \tilde{a}_4 and \tilde{a}_7 .

ROSK Model

Composition, x , for $\text{Ga}_{1-x}\text{In}_x\text{P}$:

$$x = \frac{\int \frac{d}{dt} n_{\text{InP}}}{\int \left(\frac{d}{dt} n_{\text{GaP}} + \frac{d}{dt} n_{\text{InP}} \right)}$$

Film growth rate:

$$gr = \frac{1}{A} \left[\tilde{V}_{\text{GaP}} \frac{d}{dt} n_{\text{GaP}} + \tilde{V}_{\text{InP}} \frac{d}{dt} n_{\text{InP}} \right]$$

Thickness of the SRL
(as an ideal solution)

$$d_1(t) = \frac{1}{A} [n_1 \bar{V}_1 + n_2 \bar{V}_2 + n_3 \bar{V}_3 + n_5 \bar{V}_5 + n_6 \bar{V}_6]$$

\bar{V}_i – molar volumes of the constituents in the SRL

Effective dielectric
function ε_i of the SRL:

$$\varepsilon_i(\omega) = \varepsilon_\infty + \sum_{x \neq 4,7} x_i(t) F_i(\omega) \quad \text{and} \quad x_i(t) = \frac{n_i(t)}{\sum_k n_k(t)}$$

ROSK Model Link to PRS Response

Molar concentration
of SRL constituents



Thickness of the SRL



Effective dielectric
function of the SRL



Experiment & simulated
reflectance signals

